WHY IS A MODEL TOPOGRAPHY STILL NOT DESCRIBED ACCURATELY ENOUGH AT MESOSCALE? HOW CAN IT BE IMPROVED? WHAT WE HAVE LEARNED FROM THE COMPARE EXPERIMENT

M GEORGELIN
Laboratoire d'Aérologie, UMR CNRS 354 Université Paul Sabatier
Toulouse, France
R El-Khatib
GMAP/Meteo-FRANCE
and Y Lemaitre
GMME/Meteo-France

1 Theoretical aspects

The lowest layers of the troposphere have rarely enough energy to cross obstacles the size of a mountain, the flow is blocked, its speed becomes null or reverse, therefore the air is diverted on each side of the orographic barrier, and the flow is mainly horizontal. The two branches of the flow going around the mountain form local winds. Theoretic studies of local winds creation mechanism can be found in Koffi et al.(1997), case studies in Campins et al. (1995), Masson and Bougeault (1996) The two branches reconnect on the lee side; between this point and the ridge a pair of symmetrical and counter-rotative vortices is formed. (Smolarkiewicz and Rotunno,1990) show that the first phase of vortices development is essentially inviscid and adiabatic, whereas (Schär and Durran, 1997) show how the cumulative dissipation in the wake control the dynamics of the vortices in the next phase., This theoretical view of an orographic flow at low level is illustrated in figure 1a (issued from Ölafson and Bougeault, 1996) . Numerous observations of such vortices exist, for example see Smith and Grubišić (1993).

Above the blocking level the air can cross the mountain and because the troposphere is stably stratified, the buoyancy restoring forces give rise to an internal gravity wave which propagate vertically, known as mountain wave, (figure1b). It can be demonstrated that these topographic waves transport energy upward and momentum downward. Because of non-linearity and mountain roughness this process slow down the atmosphere. The crossing flow undergo an adiabatic compression in the wave movement. A heating results from this compression, it often goes with

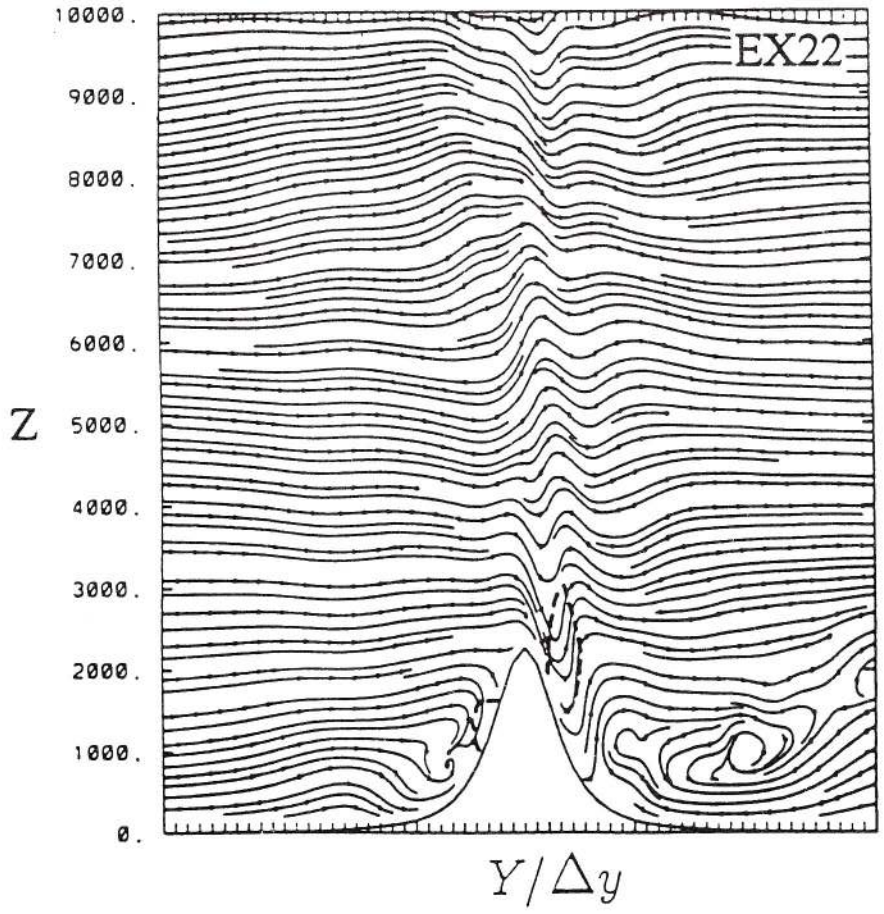
EX22
10000.
9000.
8000.
7000.
6000.
Z
5000.
4000.
3000.
2000.
1000.
0.
$Y/\Delta y$

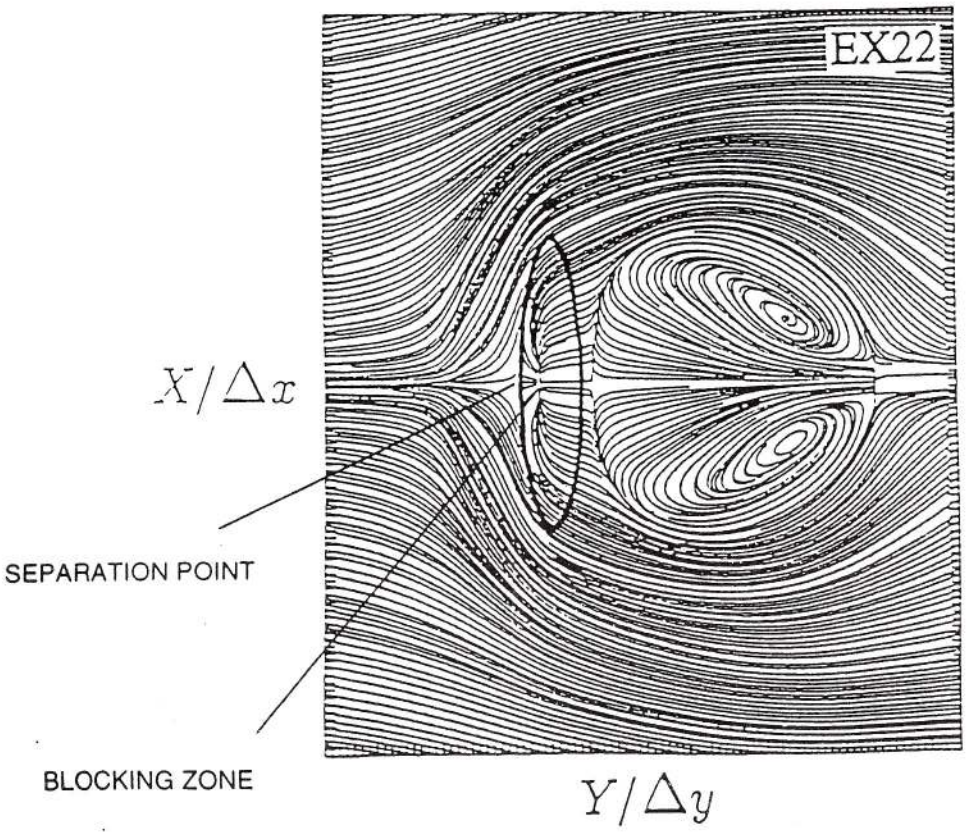
EX22
$X/\Delta x$
SEPARATION POINT
BLOCKING ZONE
$Y/\Delta y$

figure 1

strong winds this is what is called the Foehn. A deep interest has been manifested by the community on these mountain waves, see for example Durran (1990). The two aspects of the flow : -on a horizontal plane at low level, -on a 2D vertical cross section. have been mainly studied separately. But in real-world flows these two aspects are generally found together and are closely linked.

2 COMPARE

COMPARE is an acronym for Comparison Of Mesoscale Predictions And Research Experiments, for its second exercise the aim of the COMPARE group is to check the ability of existing models to simulate mesoscale orographic flows. Fifteen groups have accepted to participate to the exercise, the models and the participating institutions are listed in table 2. For this forecast and research experiment the case to choose must permit to evaluate the simulation of the aforementioned key aspects of orographic flows. The conditions were quite well filled by the PYREX experiment IOP3.

2.1 the PYREX experiment

The PYREX experiment (Bougeault et al., 1990, 1993, 1997) is a joint program of Météo-France and the Spanish Meteorological Institute, with the participation of several research institutes and funding agencies of France, Spain, and Germany. The field phase took place in Fall 1990.

The aim of the experiment was to assemble a data base to study the influence of the Pyrenean range on the atmospheric flow at meso-scale. Among the numerous phenomena of importance caused or influenced by the Pyrenean range, it was decided to concentrate on the dynamical effects of the barrier when the synoptic flow is more or less perpendicular.

In view of these objectives, the experimental set-up has been organized (see Figure 2) with a concentration of measurements over the central part of the mountain (central transect) and over the eastern edge, in order to document simultaneously the components of the flow going *over* and *around* the range. The measurements included:

- Surface parameters by 15 automatic weather stations, placed at high elevations along the central transect, including high accuracy pressure measurements, from which it was possible to compute the drag in near real-time.
- Radio-soundings at 11 stations, 4 times a day during the Intensive Observation Periods.

Table 2 : Identification of the models and experiments

Model	Institute	Identifier	Experiments
JSM	JMA	JSM	1 3
BOLAM	FISBAT	BOLAM	1 2 3
DARLAM	CSIRO	DARLAM	1 3
ALADIN	Météo-France	ALADIN	1 2
MC2	RPN	MC2	1 2 3
Europa Model	DWD	DWD or EM-DWD	1 2
Unified Model	UKMO	UKMO or UM-UKMO	1 2 3
Eta Model	NCEP	EMC or NCEP-EMC	1 2 3
RFE	RPN	EFR or RPN-RFE	1 3
Non-Hydrostatic Anelastic	JMA	NHA	1 2
SMR	SMR-ER	SMR or RER-SMR	1 2 3
HIRLAM	INM	HIRLAM or INM-HIRLAM	1 2 3
MESONH	CNRM and LA	MESONH	2
COAMPS	USNAVY	COAMPS	1 2 3
RSM	NCEP	RSM	1 2 3

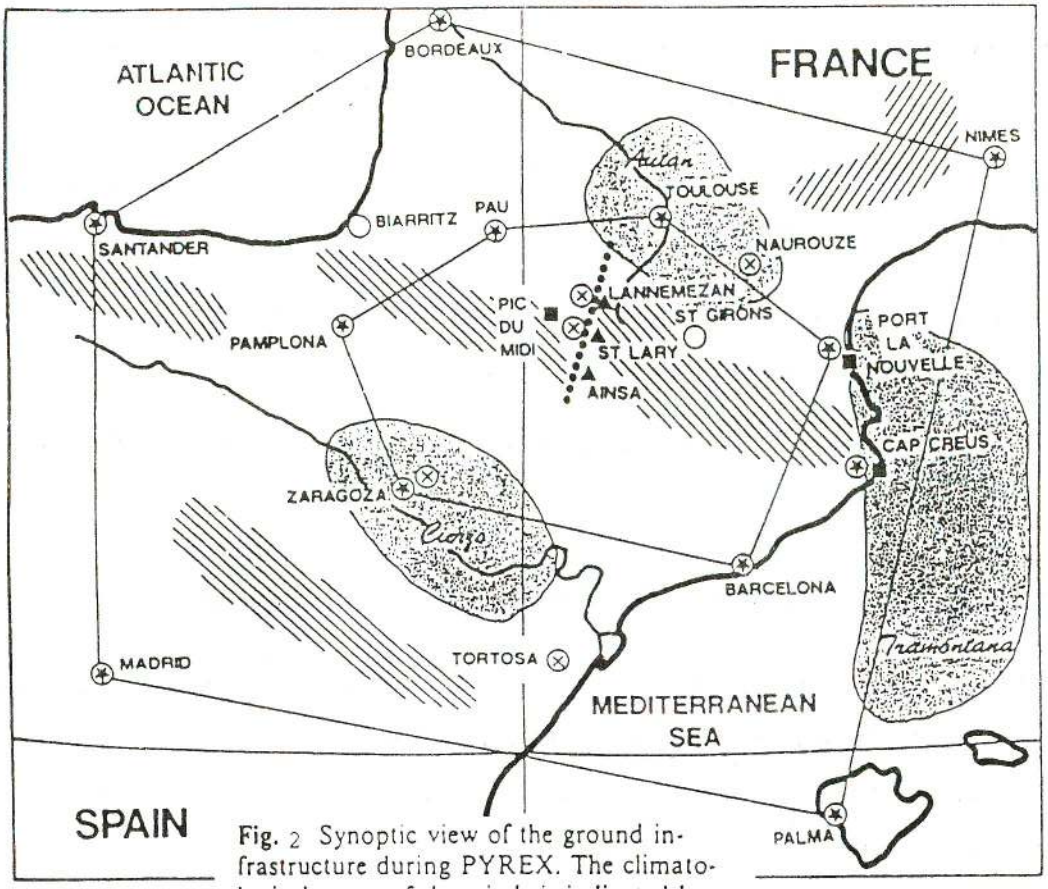

Fig. 2 Synoptic view of the ground infrastructure during PYREX. The climatological range of the winds is indicated by half-tone. ⊛ Soundings; ▲ profilers; ⊗ sodar; ● microbarographs; ■ constant level balloons

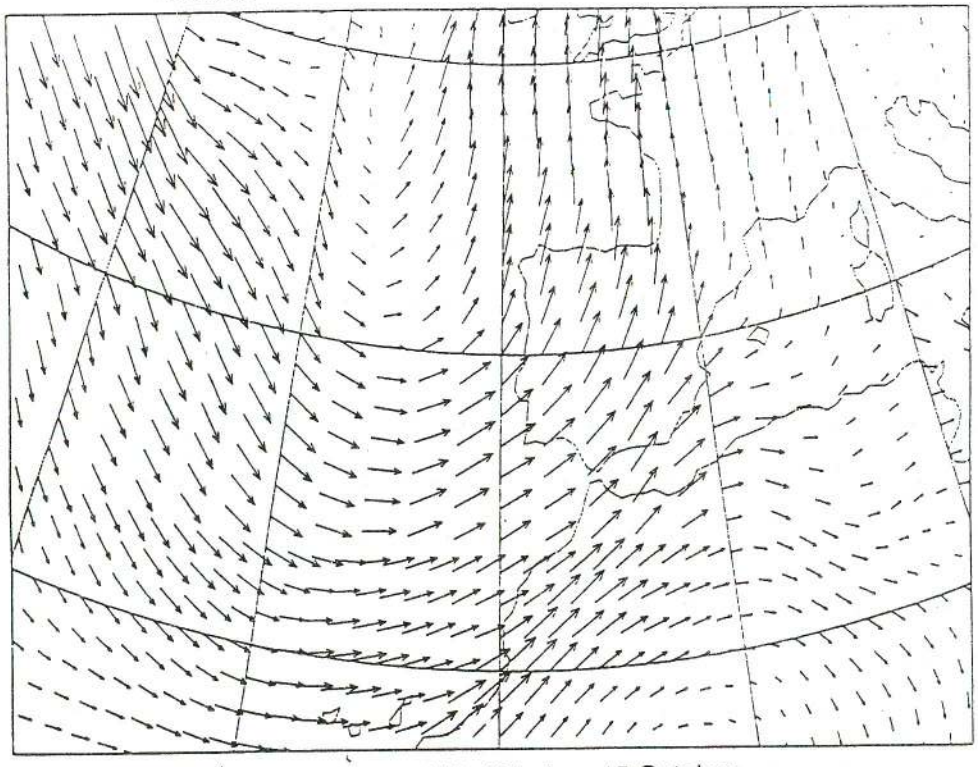

Fig 3. The 500 HPa Wind on 15 October, 00Z on the area of interest

- A network of 4 profilers, operating continuously along the central transect.
- Trajectories of constant-level balloons, both along the central transect, and around the eastern edge of the range.
- Surface measurements by a large number (over 100) weather stations, and by 5 sodars in the domain of the main regional winds.
- Four instrumented aircraft, equipped for mean and turbulent dynamic and thermodynamic measurements, flying over the main transect and around the eastern edge.
- An airborne lidar system allowing for the remote detection of the clouds and the planetary boundary layer depth.

2.2 Description of the case chosen for the 2nd COMPARE exercise

Among the various IOPs of the experiment, the Case of 3 has been very intensively studied because it corresponds to a very typical, strong lee wave event, featuring a brief peak of surface pressure drag and wave momentum flux. This is associated with significant surface flow perturbations of interest for regional forecasts.

The situation became most favourable for strong mountain waves in the evening of October 14th, due to the approach of a trough over the eastern Atlantic. This is shown by the $500hPa$ chart in Figure 3, valid at 0000GMT, 15 October. This trough directed south to southwesterly winds over the area of interest, with force reaching $15ms^{-1}$ at $700hPa$, $20ms^{-1}$ at $500hPa$, and $40ms^{-1}$ at the tropopause, just above $200hPa$. The core of wind maximum was drifting slowly to the east during the whole IOP. At the peak intensity of the event, during the morning, a full description of the mountain wave by three aircraft flying simultaneously is available. the pressure drag across the range during the whole period is also available, (Bessemoulin et al. 1993).

During the whole period, the area of Toulouse was subject to the classical "Autan" wind, reaching a force of about $15ms^{-1}$. It is limited to a shallow layer below a strong inversion. Other places in the Pyrex area had very weak wind, due to a shelter effect.

Finally, one of the most interesting aspects of the surface wind field is the formation in the early afternoon of 15 October of a small scale lee vortex pair (about 100km in diameter). These vortices also drifted slowly towards the west, and were documented by the surface meso network, and by the Lannemezan Sodar.

The event intensity decreased during the afternoon, whereas the south-west flow was still present in altitude.

Unfortunately the available observations do not allow a reliable study of the foehn heating and the upwind blocking. aspects could not be studied. For the evaluation of the mountain wave, lee vortices, local winds and pressure drag forecast the simulation domain

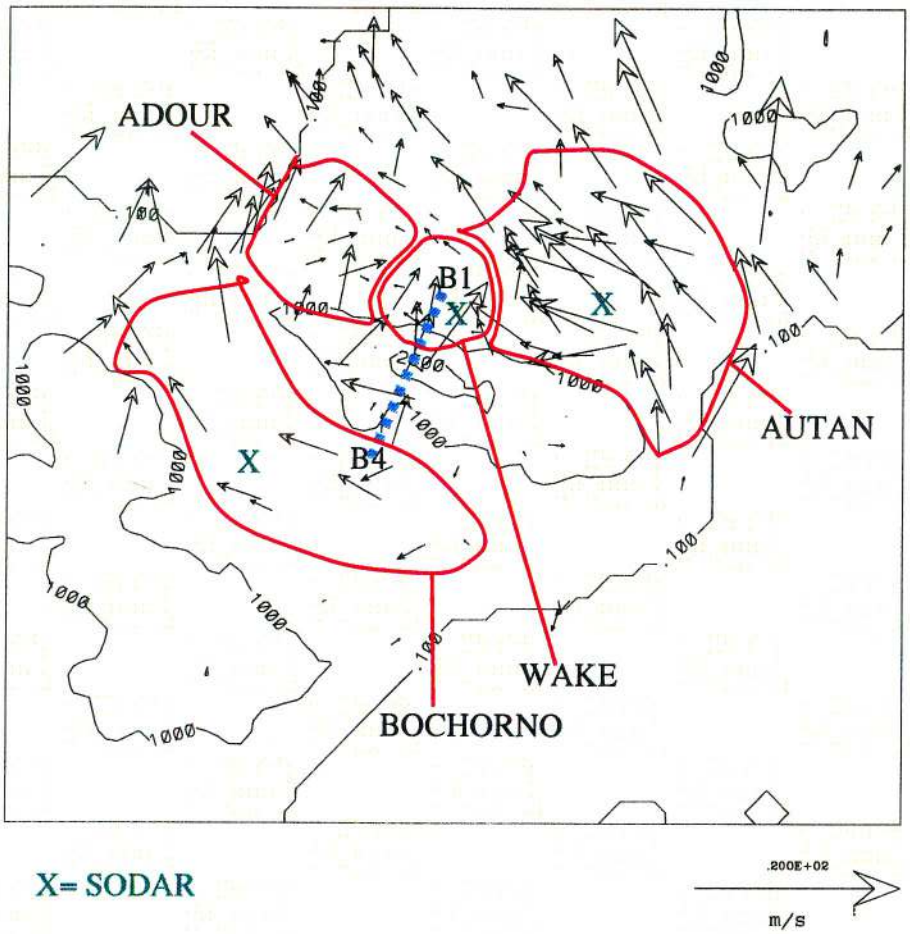

figure4

has been shared in different geographic areas presented in figure 4. an area is devoted to the vortex study and it surrounds the zone of the return current of the vortex pair as it appears in the observations. In the same area, at Lannemezan, there is a sodar which gives a description of the vortex structure between ground and 350 m. For the Autan wind the zone corresponds to the location of the so-called local wind. A sodar in the same area gives additional information on this wind. for the Bochorno the area surrounds the Ebro valley, there is also a sodar into this

area. And finally the "Adour" area go with a so-called valley. The "Adour" zone, as it will be seen further is fed by air which crosses the mountain. From 10 to 25 ground stations are located in each of these sub-domains. Along the line B1B4 three planes have flown along 10 different legs, and given a good description of the hydrostatic wave between 615 and 197 hPa. Still along this line, 14 microbarographs have permitted to calculate a very reliable pressure drag.

All participating models have been evaluated at the same place where the measurements were done. Scores have been calculated for all domains as for the planes and sodars. The scores we use are the Root Mean Square error and the bias. We have the relation:

$$RMS^2 = b^2 + \sigma^2$$

with $b = \overline{Forecast - Observation}$ the bias

and $\sigma = \frac{1}{N}\sum_i^n((F_i - O_i) - b)^2$ the standard deviation of error.

the RMS could be understood as the "total error

RESULTS

3 Experiment 1

Experiment 1 has been the one with the more participants (14). It has been run on a domain close to the one presented in figure 2, with a 10 kilometer resolution, this experiment is clearly a forecast experiment and the results should not be influenced by the analysis except for the initial state. The comparison will be presented in a way to illustrate the main characteristics of orographic flows as discussed above.

3.1 Local winds

At low level, the flow which impinges the Pyrenees splits into two branches: the eastern one goes around the mountain and forms the Autan wind, it is further re-accelerated by the narrowing between the Pyrenees and the Massif Central, the western one is canalized by the Ebro valley and forms the Bochorno (see figure 4).

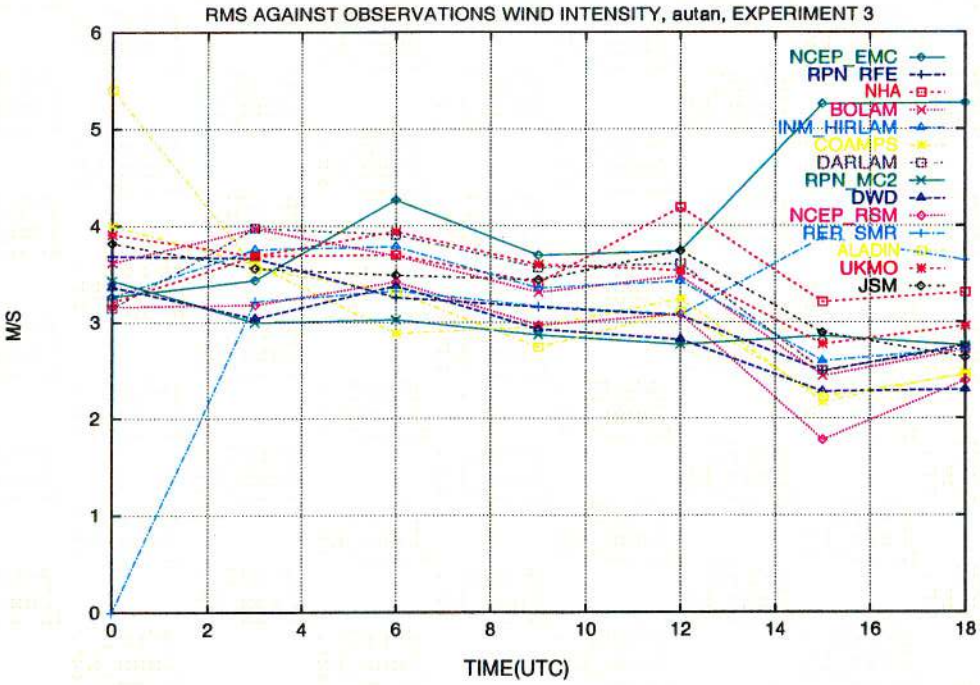

figure 5

Figure 5 displays the Time evolution of Root Mean Square error for the wind intensity of the Autan wind. This figure should be considered relevant after 3 UTC, since the experiment begins at 0 UTC, and three hours should be the time for the models to adapt to initial conditions. The Autan error should not be considered either on and after 15 UTC because its area is polluted by the wake circulations. Taking into account the above restrictions, One can observe that the value of RMS is stable with time for the Autan, around 3.5 m/s, the error is more variable for the Bochorno but it remains equal to or under the Autan value.

Figure 6 shows the corresponding bias for the Autan wind and the Bochorno. A negative bias means that the simulated wind is weaker than the observed one. One can notice that, for both winds the bias is found negative for all models except the NCEP-EMC and RER-SMR for the Autan (yet, their RMS or total error is the same as for the others). Concerning the Autan wind direction, on the whole the models have a negative bias which signifies here that the forecasted winds are too much north. Since this wind rotates around the edge of the mountain, his curvature radius is function of its speed and this may explain the correlation between the wind strength and wind direction. In contrast, for the Bochorno wind, the bias is found around zero, which was expected because this wind is canalized into a valley. To understand this general behaviour of the models, it is useful to look at scores in the Adour zone (figure 7). This zone is downwind of the mountain and in figure 4 one can see that this area is fed by the part of the flow which

goes above and across the Pyrenees. It is also the area where the (observed) Foehn begins.

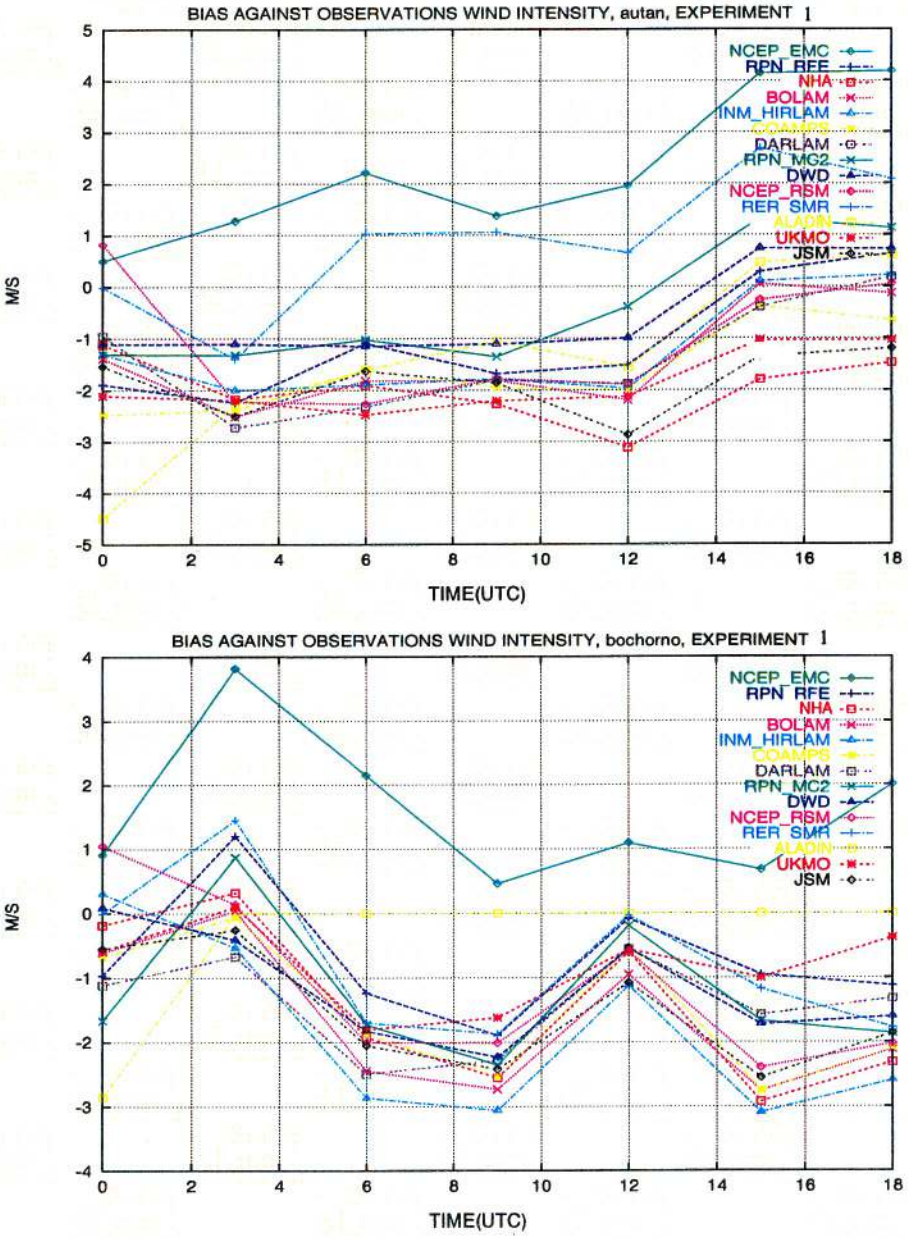

figure 6

On this picture one can notice that, on the whole, model bias are positive for the wind intensity, and this means that the predicted part which goes above the mountain is stronger than the observed one. This behaviour highlights the local wind scores: If local winds are too weak, it is because the part of the flow which is going above the mountain is too big with respect to the part

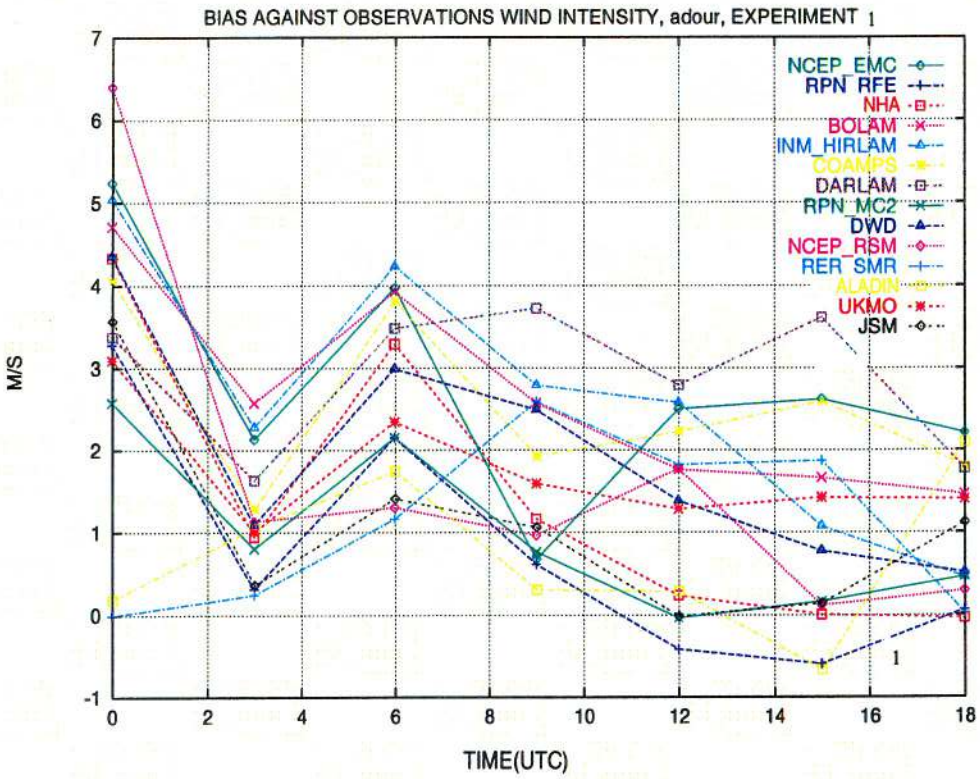

figure 7

going around it. The blocking appears to be insufficient.

3.2 Lee vortices

The sketch of picture on figure 8 represents the time evolution of the observed surface wind, on it can be seen the appearance and disappearance of the pair of lee vortex. At 12 UTC some northern winds (i.e reversed winds) appear downwind near the center of the Pyrenees, it is the return current of a pair of counter-rotative lee vortices. At their maximum, at 15 UTC, their width is about one hundred kilometers. At 18 UTC, in the center of the mountain, the wind has turned to south, west of the range some smaller vorticity is found. Between 15 and 18 UTC the lee vortices have shrunken and moved westward.

Figure 9 shows a comparison with the Lannemezan sodar results: the first row corresponds to the observation at 15 UTC between ground and 350 meters, the other rows correspond to the simulated wind, at the same location and same time, for each participating models. The observed northern wind is the signature of the return current of the two counter-rotative eddies, only two models (out of fourteen!) can reproduce this observed reversed wind. Looking at wake winds scores and models surface wind fields, it appears that half the models have no vortex at

all at 15 UTC, for the others the vortices sometimes appear too early, are not located at the right place and are in general over developed at 18 UTC.

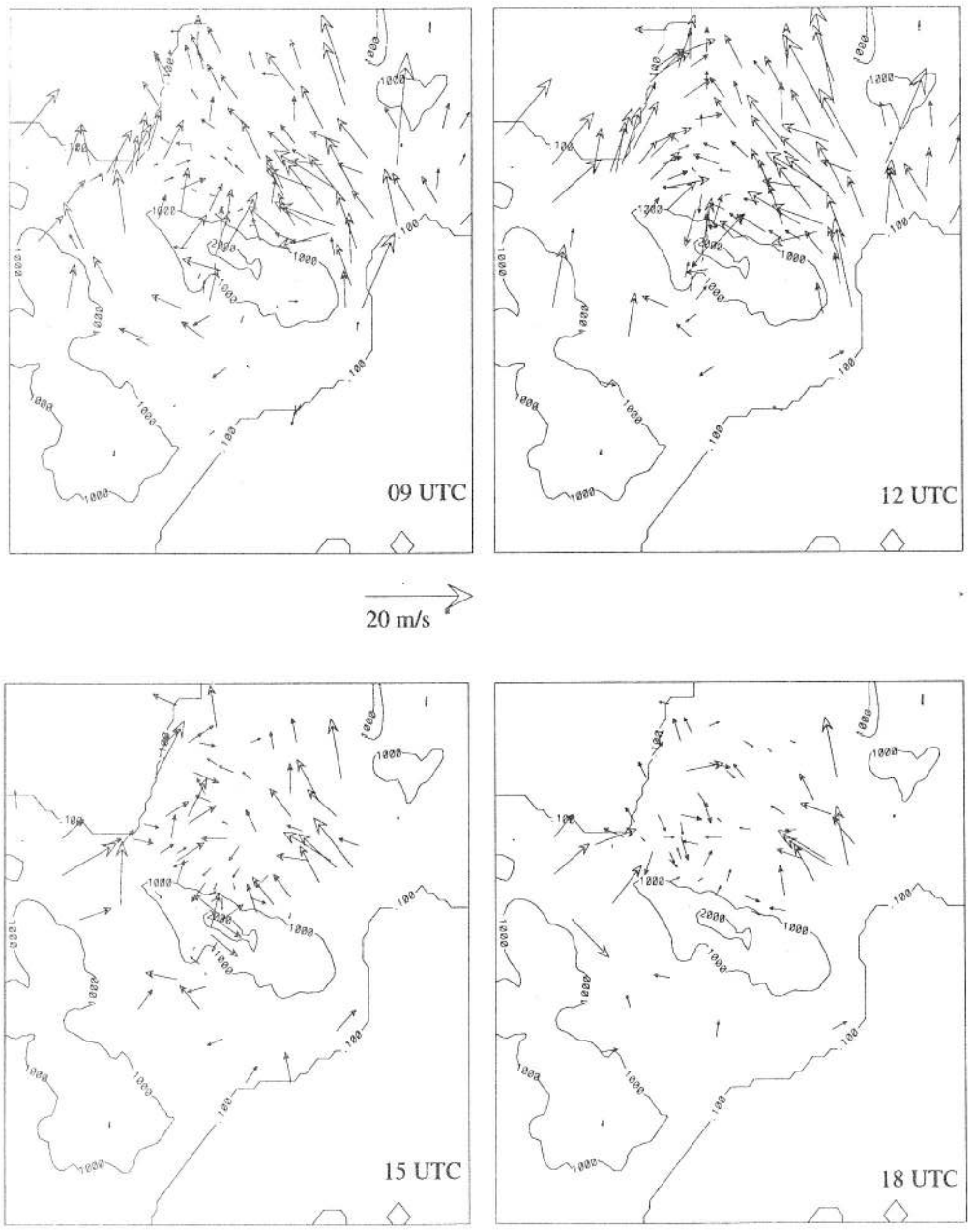

figure 8

This bad forecast may be linked to the poor representation of bocking yet mentioned.

3.3 Mountain Wave

Between 6 and 9 UTC, three planes have made 10 different pressure legs. Scores have been calculated for each leg for potential temperature and the wind component perpendicular to the ridge. The RMS for the cross-mountain wind component, is around 5 m/s except around 350hPa

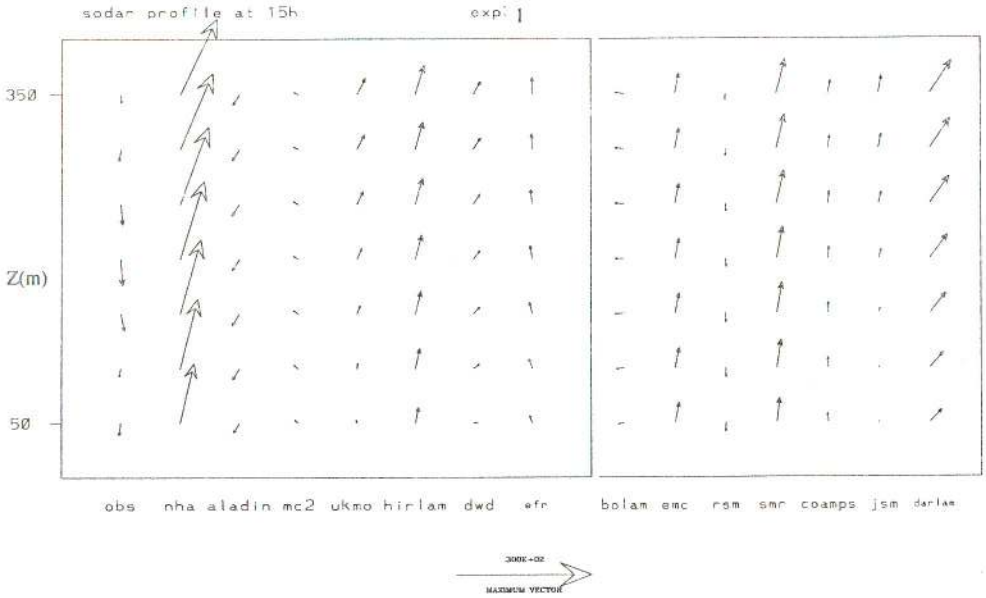

figure 9

where all models show a bigger error. The error in potential temperature is around 2 Kelvin at low level and increases with altitude up to 6 Kelvins at tropopause. Looking at models results along a pressure leg allow us to better explain these scores. Figure 10 shows the ARAT 545hPa leg for cross-mountain wind and temperature. The observed and simulated variables are presented together along the flight track which is about 200 kilometers long. For the wind, one can see that at the upwind edge, all models have stronger winds than observed. A part of the model error is due to this discrepancy but the major part of the error comes from the over-estimation of the wave amplitude for the majority of the models. The temperature picture also shows the over-estimation of the simulated waves, but it does not seem to present any bias at the upwind edge. There is not enough air which is diverted around the Pyrenees, thus there is too big a part of the atmosphere which crosses the mountain participating in that way in the mountain wave mechanism. It is coherent with the fact that the wave amplitude is in general over-estimated.

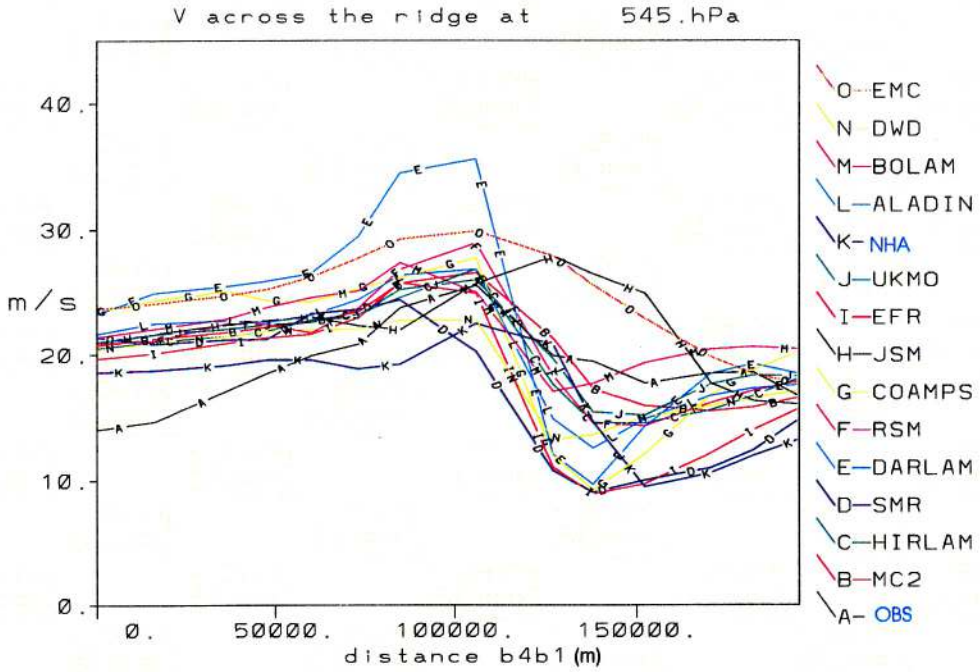

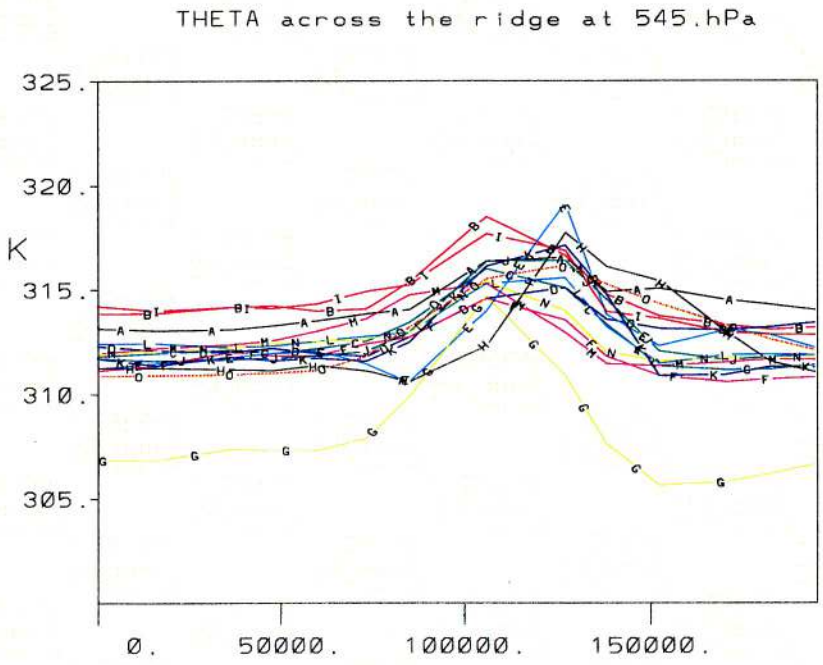

figure 10

3.4 Pressure Drag

In the PYREX experiment, the drag was evaluated following (Bessemoulin et al., 1993):

$$D = \frac{1}{L} \int_{Zdown}^{Zup} \Delta P(Z) dZ$$

Where D is the drag, P the pressure, Zup the altitude of the ground station at the upper level, $Zdown$ the altitude of the ground station at the lower level. $\Delta P = Pupwind - Pdownwind$

at the same altitude Z. In each model the predicted drag has been evaluated at the location of the microbarographs. It can be demonstrated in the linear case that the drag is a measure of the action of the mountain on the atmosphere and is directly related to the wave induced perturbations (Eliasen and Palm, 1960). Figure 11 represents the time evolution of the pressure drag .

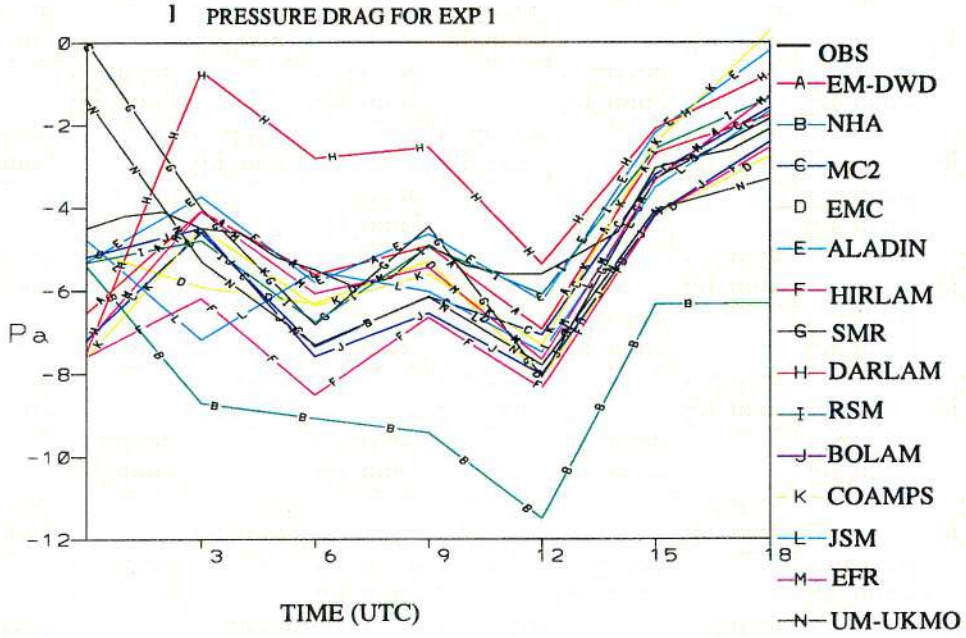

figure 11

The mountain Drag is negative here because the IOP3 is a southern flow. One can observe that the simulated pressure drag is generally stronger (in intensity) than the observed one, except for one model which stands out from the rest. But some models give a drag which is remarkably close to the experimental one, because drag is a second-order variable and therefore difficult to reproduce. The time evolution of the drag is generally well simulated. The pressure drag represents a diagnostic of the wave intensity, the drag value of the various models should therefore be correlated with their ability to represent the wave field. But looking at figure 10 with figure 11, it surprisingly appears that model drags do not seem to be corelated with the wave amplitude.

3.5 Discussion

If we suppose that the relief is the essential forcing of this flow, the main cause of bad forecast is the lack of precision in the topography definition.

- The insufficient blocking should be related to the the difference of height between the 10km orography and the actual relief (more than 500m at the summits).
- The fact that the mountain wave amplitude is too strong indicates that the mountain is not slowing down enough the crossing flow. It suggests that the roughness of the mountain is under-estimated.

To confirm these assumptions we should eliminate another source of error which could come from the larger scales. The experiment 1 lateral boundaries are driven by a larger scale forecast (which will not be described here), which a priori contains errors. Another experiment has been conducted with a modified protocol which add to the experiment 1 configuration a large scale forcing applied every six hours at the simulation domain boundaries. This forcing is provided by the ECMWF analysis.

4 Experiment 2

Thus experiment 2 should be rather considered as a dynamical adaptation than a forecast experiment. 12 models have performed this experiment of which 11 have also done experiment 1.

4.1 Local winds

The RMS and bias of local winds calculated from experiment 2 results reveals that, for the majority of the models, there has been no improvement from experiment 1 to 2. The same is found for the wind direction of both winds. A change in the large scale forcing does not modify the local winds RMS, hence it can be said that local winds details are mainly determined by the mesoscale mountain.

4.2 Lee vortices

The simulation of the wake gives different results from experiment 1, The way lee winds weaken and turn south, is mostly common to the models participating in experiment 2, and signify that there is a trend to form vortices. Models which have already wake eddies in experiment 1, have them now stronger and located at a more correct place. In a global view the forecast of the wake is still not a success, nevertheless a few models are doing now quite a good job in

simulating correctly the lee vortices as they are at 15 UTC but all models still fail in describing the evolution of the vortices between 15 and 18 UTC.

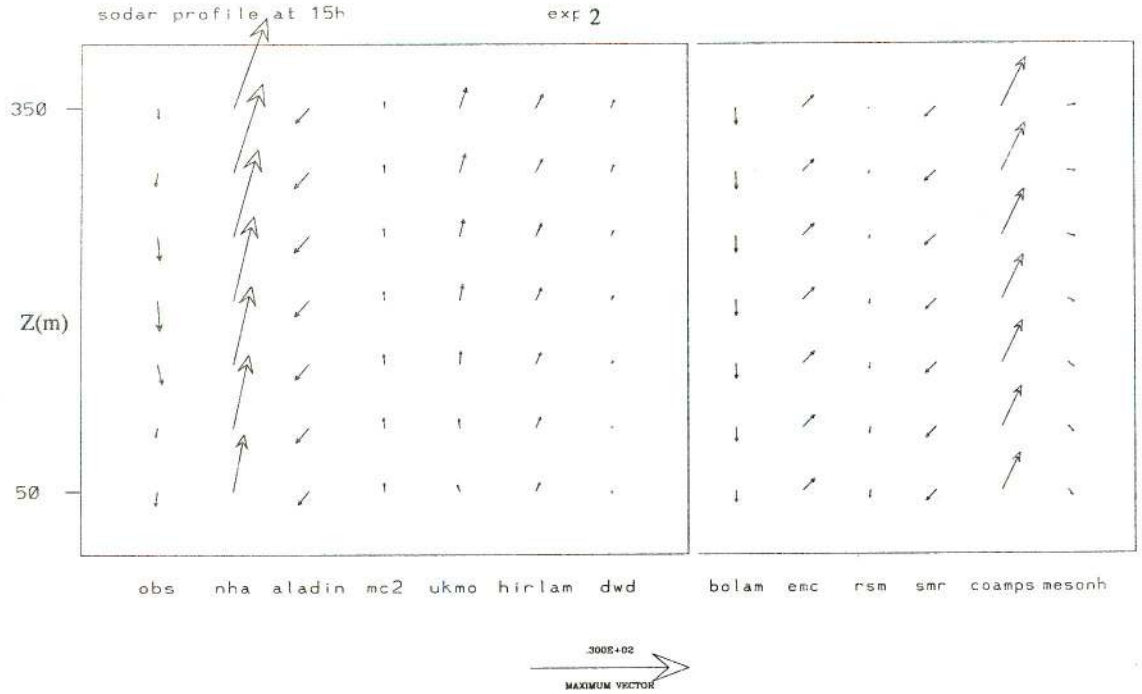

figure 12

Generally speaking the wake simulation has been improved by the improvement of the large scale forcing; as it can be verified comparing figure 12 with figure 9.

4.3 Mountain Wave

Figure 13a presents a comparison between the models and the observation at the 483hPa plane leg for the cross-ridge component of the wind. Comparing this figure to the equivalent for experiment 1 (figure 13b) leads to two remarks: the wave amplitude is globally the same. and: in experiment 2 models are more grouped, (it keeps true for other legs). From the first remark one can deduce that no general improvement is produced by the addition of a more correct large scale forcing, on the other hand the second remark indicates that models which were too far from the mean behaviour are gathered with the others by the effect of the large scale forcing. All this brings to light that, indeed, the forcing due to the

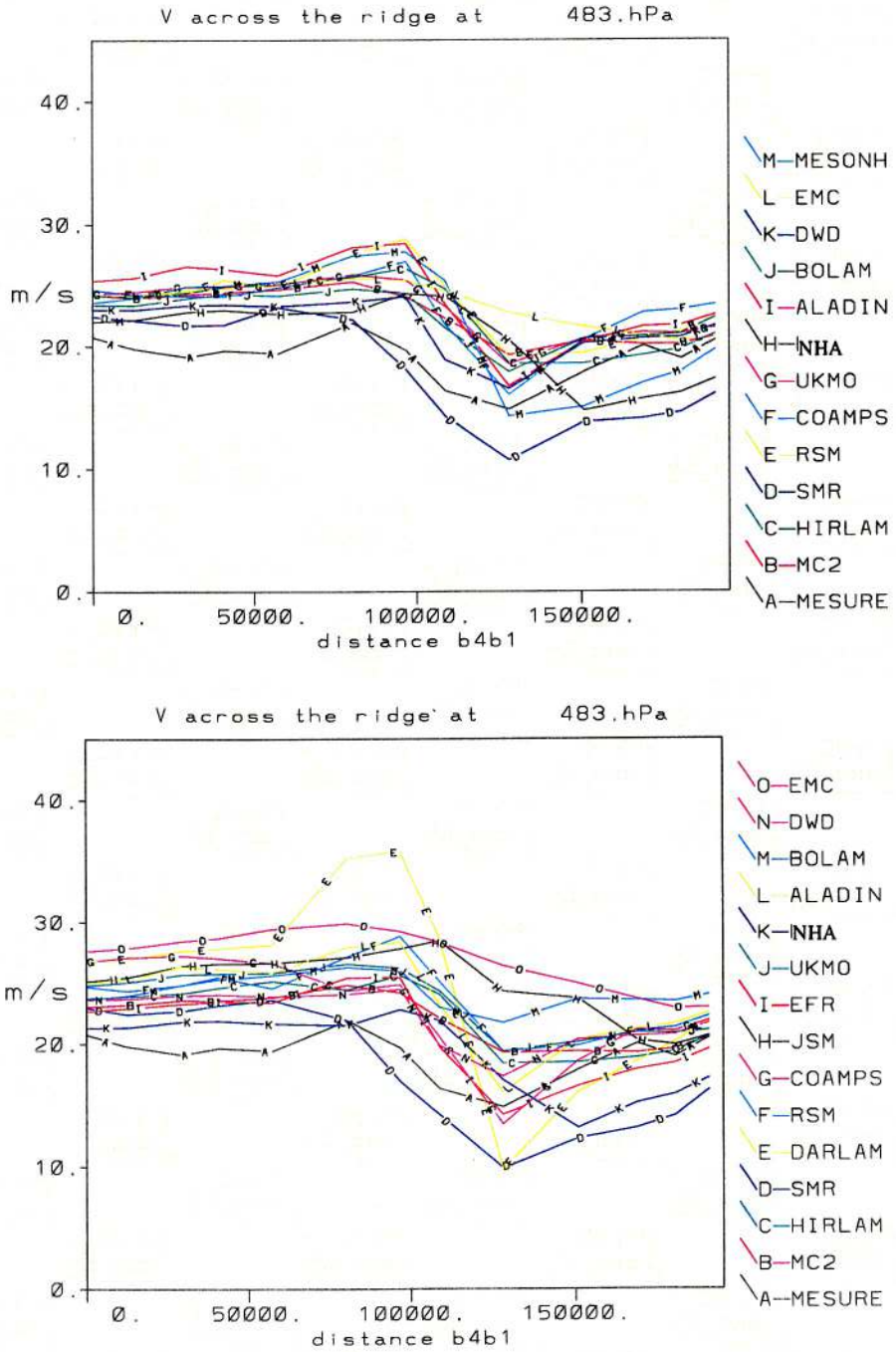

figure 13

topography is mainly responsible for the RMS since the large scale forcing is unable to correct the error on the wave but the fact that the models are more grouped reveals that there is an effect of the large scale forcing on a small scale feature like a mountain wave.

4.4 Pressure Drag

The pressure drag comparison (not shown), oddly enough, give a more scattered repartition of the different models and seems thus to disagree with the aforementioned conclusions. It confirms the fact that there is no obvious link between the wave field (between 615 and 197hPa) and the pressure drag.

4.5 Discussion

Experiment 2 results indicate that the large scale do influence small scale features, such as the wake of a mountain, and the mountain wave. The introduction of a forcing by the analysis improves the wake forecast it also permits to avoid that the simulated waves depart too much from the observation. Except the wake, there is no general improvement from experiment 1 to experiment 2. Experiment 2 have thus permit to eliminate the deficiencies due to the absence of a correct large scale influence. It reveals that the fact that the wave amplitude is over-estimated and that the local winds (and blocking) are under-estimated should be mainly attributed to the inaccuracy of the topography representation , even with a 10km grid mesh.

Some recents works produced as part of the PYREX experiment lead us to examine two different ways of parameterizing the subgrid orography, which could compensate the model topography deficiencies. Bougeault et al.(1992) have found that the use of an envelope topography ($Z_{env} = Z + \sigma$, where Z is the relief altitude and σ the standard deviation of the topography), on the IOP3, is necessary to obtain the good pressure drag, i.e the right force exerted by the mountain on atmosphere. They found that a one σ orography enhances the Drag of 66 percent but another positive effect is the enhancement of the blocking and thus the acceleration of the diverted air in both side of the mountain. The maximum intensity of the Autan wind is found to be increased of 2 m/s. On the other hand Georgelin et al (1994) have shown, on the same IOP, that the use of an effective roughness length, representative of the subgrid friction, (see Mason (1986)), in a mesoscale model leads to the improvement of several aspects of the flow. With an effective roughness length, reaching 17m over the Pyrenees summits, the mountain wave amplitude is much more accurate, the blocking is intensified, the wind direction and the lee slope turbulence seem also to be slightly improved. These two results have guided the design of the third experiment: An envelope orography (one σ) plus an effective roughness length equal to $\frac{\sigma}{80}$ (maximum value around 8m) are prescribed for each participants; the other conditions remain those of experiment 2.

Before looking at experiment 3 results, we can already have an indication of the parameterization efficiency by looking at table 1. From the ten legs of the plane measurements, weighted global scores have been calculated for the potential temperature and the cross-ridge wind. In table 1, all the participating models are classified with respect to their score in potential temperature and cross-ridge wind. It reveals that the models which are the most successful in reproducing the IOP3 mountain wave are those which use an effective roughness length, together with a mean orography. Therefore the envelope orography parameterization does not appear to be the right choice for simulating accurately the wave field.

5 Experiment 3

Eleven models have been participating in experiment 3. of which eight have done experiment 2, for seven of them, the topography has changed from a mean orography to an envelope orography, (one had it already). The maximum height of the mountain is then increased of about 500m.

An improvement of the forecast was expected from the design of experiment 3.

5.1 Local winds

It is found that there is no progress from experiment 2 to 3 the bias against the Bochorno wind intensity can be even considered as worse than in experiment 2 (and 1) (figure 14). The same result is found for the Autan wind intensity, the diagnosis of the error remains the same: the local winds are too weak. The envelope orography proves unable to enhance the local wind intensity.

The Adour region whose flow is considered as fed by the air crossing the mountain gives different results from experiment 2 to experiment 3. In experiment 3 the bias (and the RMS) is smaller than in experiment 2 (of about 1 m/s in average) between 3 and 12 UTC. It indicates that there is less air which is crossing the mountain than in experiment 2. This time the envelope orography seems to behave as expected, the blocking is enhanced. The examination of surface wind fields confirms that point

Table 1 : Global scores against planes measurements

theta (O)	V(X)	Mean orography	envelope	Zoeff
EFR	DWD-EM	X O		X O
MC2	UM-UKMO	X O		X O
EMC	MC2	X O		X
UM-UKMO	EFR	X O		X O
ALADIN	HIRLAM	X	O	X O
HIRLAM	BOLAM	X O		X O
NCEP-RSM	ALADIN		X O	X
DWD-EM	JSM	O	X	X O
NHA	NHA		X O	
BOLAM	RSM	O	X	O
SMR	COAMPS	X O		
DARLAM	SMR	X	O	
JSM	EMC	X	O	O
COAMPS	DARLAM	0	X	

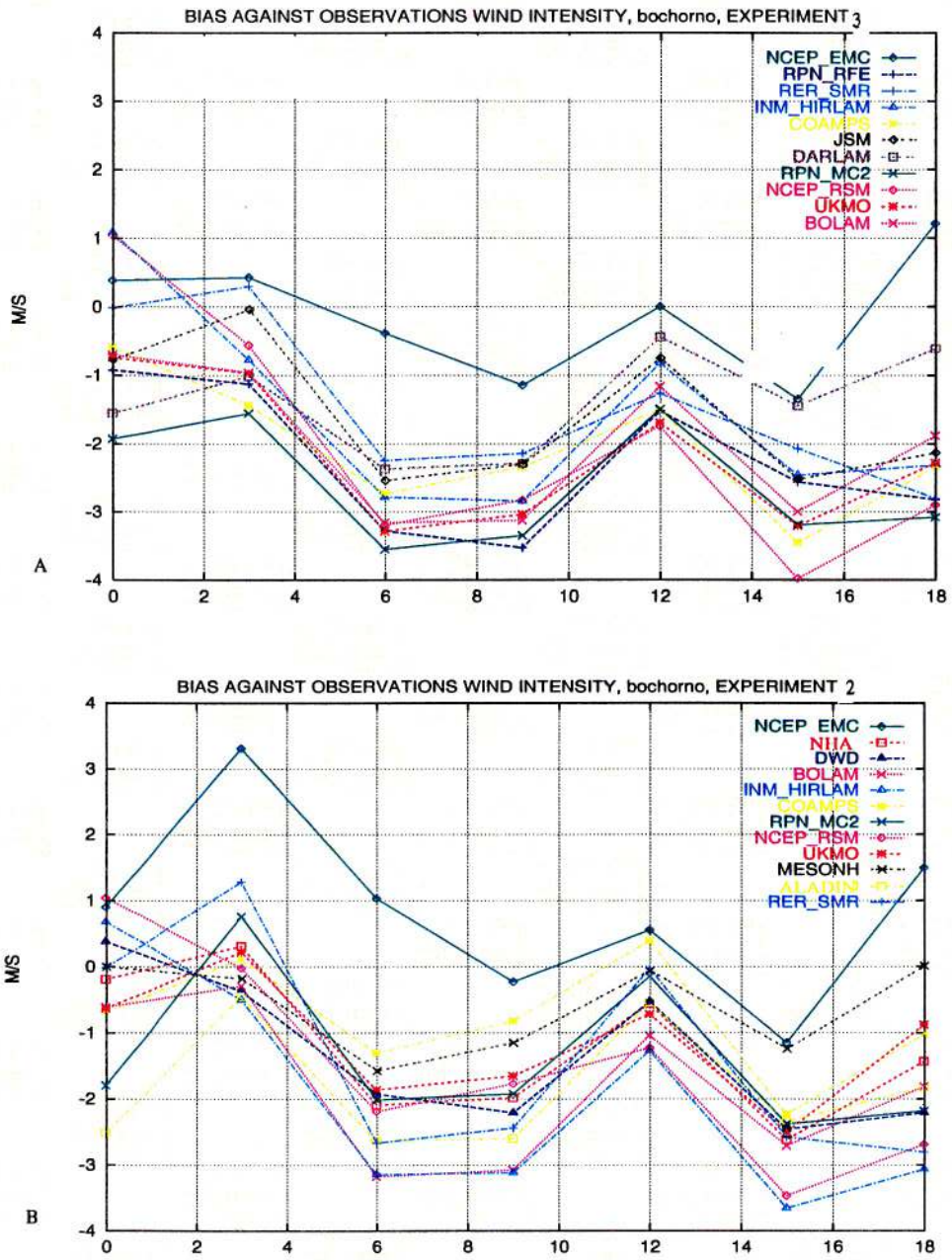

figure 14

An explanation to these paradoxical results could be that the envelope orography parameterization smoothes the topography and "fills" the bottom of the valleys, therefore the narrowing between the Pyrenees and the Massif Central disappears as well as the Ebro valley becomes less deep. The mechanism of acceleration of these winds due to a Venturi-like effect is then less efficient. However the result only concerns surface wind, and the wind could have been enhanced in the middle of the PBL.

5.2 Lee vortices

figure 15 presents a comparison of the Lannemezan sodar simulation between experiment 2 and 3, at 15 UTC. The improvement is spectacular: concerning the seven models whose topography has been changed from experiment 2 to experiment 3, for three of them a reversed wind appears in experiment 3, for two of them the wind is strongly reduced, and for the last two models the wind profile remains the same but they were correctly already simulating the reversed wind in experiment 2. On the whole eight out of eleven models have been able to reproduce a reversed wind at the sodar location with an envelope orography together with an effective roughness length.

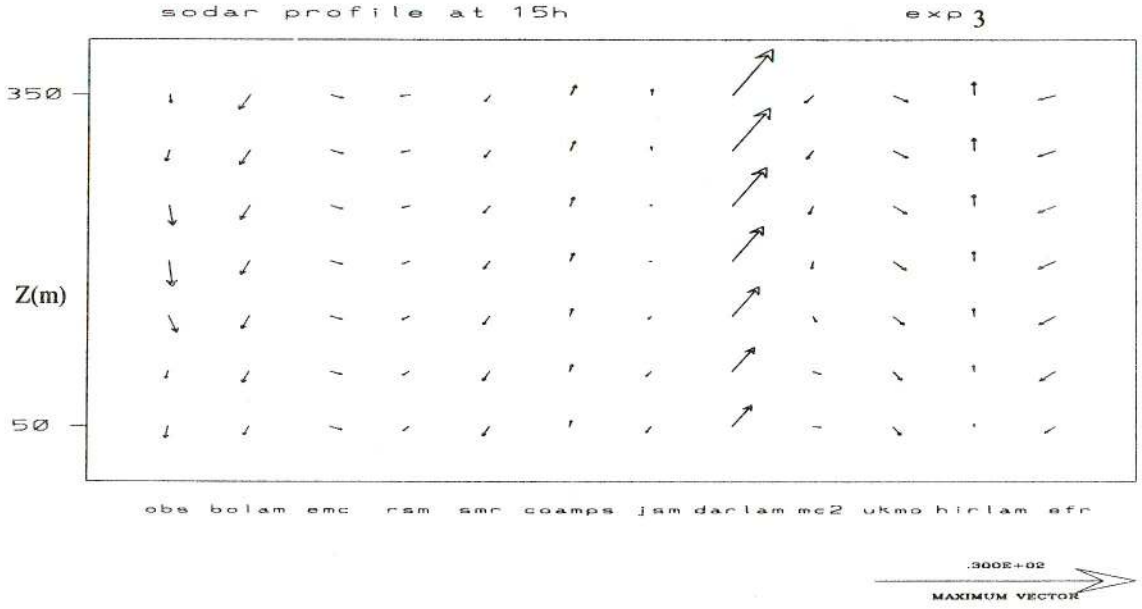

figure 15

In fact looking at the surface wind fields indicates that lee vortices are present in all models but not every time with the right location or the right extension.

A RMS error can be calculated from the sodar wind direction. The difference between experiment 2 and 3 scores, is that experiment 3 show stronger errors at 6 or 9 UTC. It signify, in fact that in some models the lee vortices circulation appears too early.

With respect to the vortices, the topography height increase and its resulting higher blocking are upwind modifications. The fact that in experiment 3 the vortices simulation is in progress signify that the lee vortices development is controlled by the upwind characteristics of blocking.

5.3 Mountain wave

The scores against the plane measures are worse than for the previous two experiments. For the lowest legs the mean RMS of the models for the wind is found about 1 m/s bigger than in experiment 2. The reason of this degradation is obvious when looking at figure 16, the wave amplitude is globally higher in experiment 3, than in the previous experiments. It was expected that the increase of the height of the mountain would enhance the blocking, it seems to be the case, but it also leads to the enhancement of the mountain wave amplitude. This underlines the non-linear character of this type of flow.

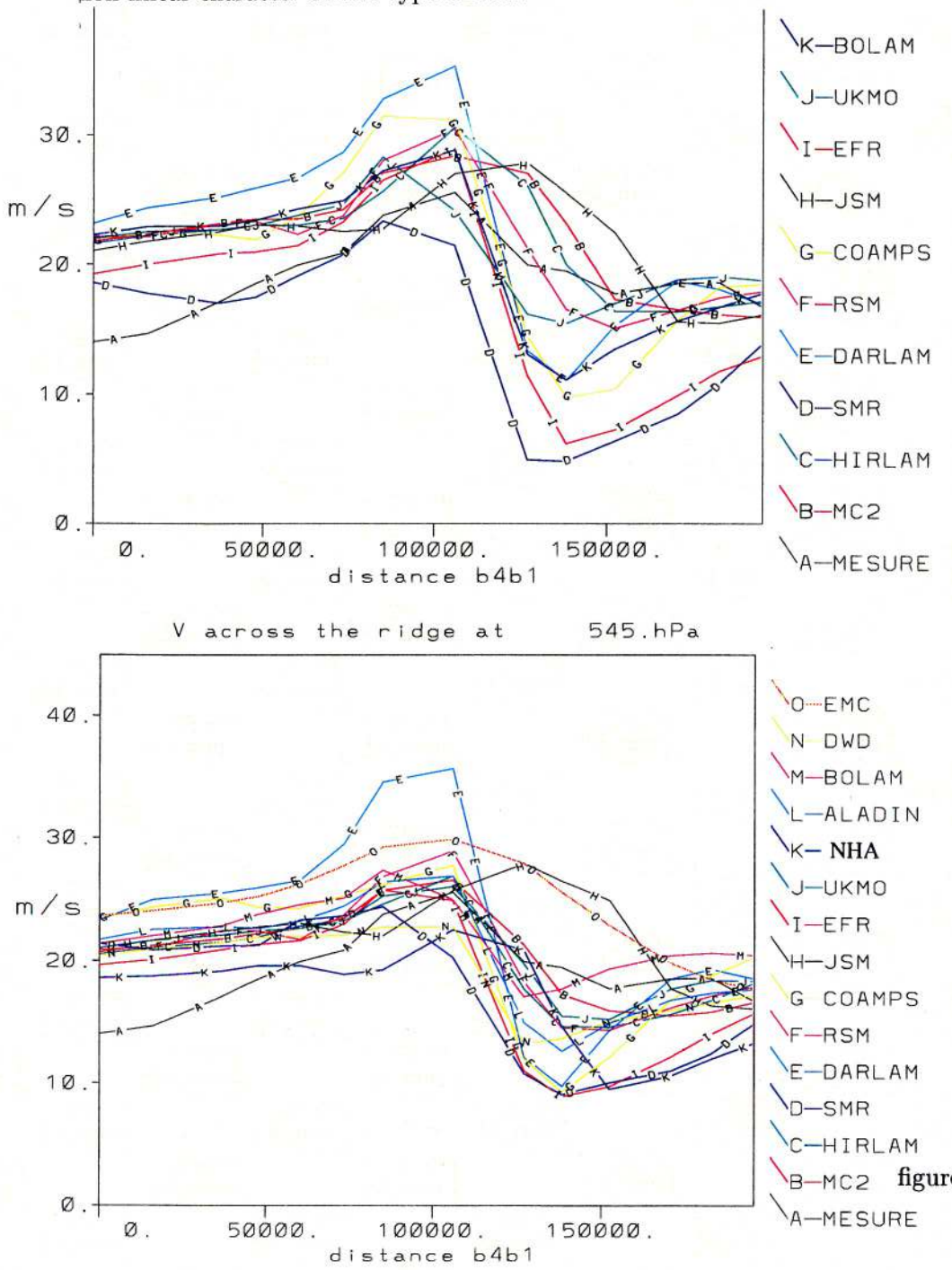

figure 16

5.4 Pressure drag

One can notice that the mean of the models is lower than for experiment 2 As the development of lee vortices in a general way is the main characteristic of experiment 3, the global decrease of the pressure drag comparatively to the other experiment is obviously the fact of the wake circulation. Looking back to the drag figure of experiment 1 (figure 11), one can notice that models with the best drag at 12 UTC (and 9) are the two which give the right lee vortices.

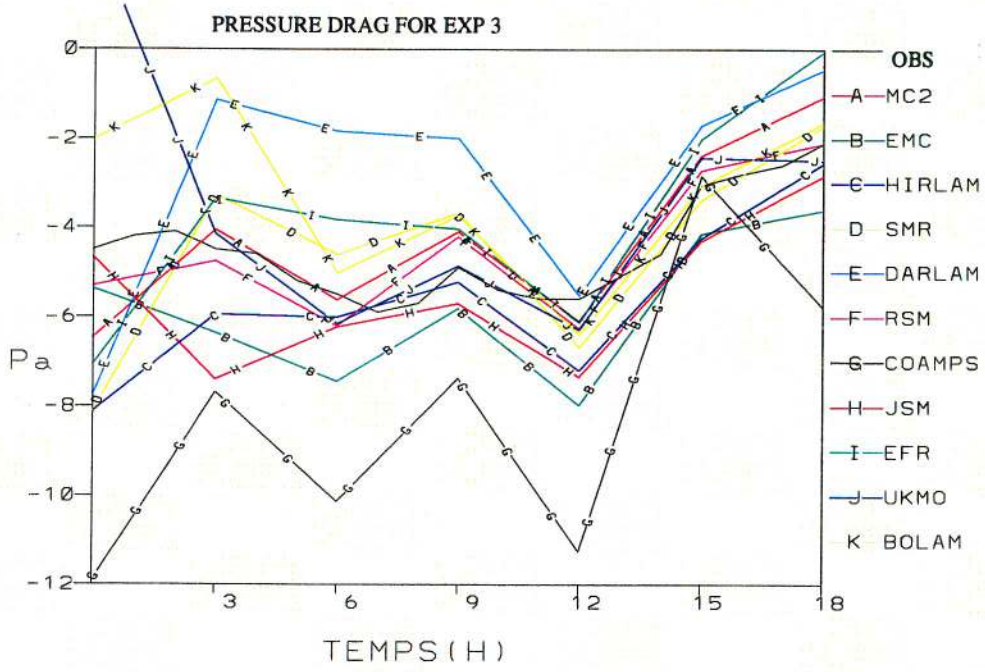

figure 17

When the wake evolves towards a pair of lee eddies, in its center first the wind is reduced and then becomes reversed and forms the return current common to the two lee vortices. If the wind is reduced or reversed [2] the pressure increases downwind and thus the cross-ridge pressure gradient, source of the drag is reduced.

From these three experiments it can be considered that the drag is definitely unsensible to the wave variations since it has been shown just above that the wave amplitude is again too strong in experiment 3.

5.5 Discussion

Globally the prescribed configuration has not been able to improve the forecast of the IOP3. The only positive action of the envelope orography parameterization has been to favour the

[2] because it advects colder air

appearance of the lee vortices. Nevertheless one can notice that an envelope may not be necessary to get the correct wake, since the BOLAM model has succeeded in its simulation in experiment 2.

Due to the only 0.01 degree resolution of the relief DATA and the 1 σ choice, the prescribed envelope is low among other choices of envelope calculation but the local winds improvement calls for a higher mountain. Inversely for a more correct time of appearance of the lee eddies, a smaller relief highness is required. A higher orography will also enhance again the wave amplitude.

The roughness length with a maximum of 8 meters does not seem able to compensate the wave enhancement due to the higher relief. In experiment 1, models giving the best wave have it around 20m. With an envelope orography the roughness length value should be again bigger, but it is limited by the model first level height.

The envelope orography parameterization was first calibrated to give the right pressure drag across the mountain in large scale models, (Clark and Miller, 1991), at mesoscale the parameterization follow the same concept (Bougeault et al., 1992); yet the COMPARE results reveal a strong link between the pressure drag and the wake vortices circulation (since the drag computation is done on the recirculating area) and no obvious link with the above mountain wave. The usefulness of the (2D) drag as a diagnostic, and the validity of the envelope orography parameterization are then questioned.

6 Summary

The COMPARE experiment results, at mesoscale emphasize the fact that the orography representation with a 10km mesh is still not sufficiently close to reality for accurately forecast an orographic flow at mesoscale.

-The discretized mountain does not create enough blocking at low level, it results from this that the local winds intensity are too weak.

-The model topography does not slow down the atmosphere enough that is why the mountain wave is too strong.

The COMPARE experiment also shows that at mesoscale although the topographic forcing is preponderant a good large scale forcing is still useful since it ameliorates the wake simulation and prevents the simulated waves to depart too much from reality.

An ideal parameterization should be able to represent the effective blocking of the topography and its effective subgrid roughness. Results from experiment 3, on local winds, suggest that the details of orography should also be represented (canalization into valleys ...). The effective roughness length parameterization is able to correct the lack of roughness of the model orography. The envelope orography parameterization should not be retained since its balance is rather negative. An alternative like the silhouette orography should also be evaluated.

The blocking effect and the local winds have not been corrected by any of the proposed solutions. A new parameterization (Lott and Miller,1997) which represents the boundary layer dissipation within the gravity wave drag parameterization, could give better results and improve the blocking effect because the subgrid friction is distributed on all the level below a parameterized blocking height. It may represents in the same time, the right roughness intensity and the right barrier effect.

Acknowledgements

The COMPARE experiment was made possible by the participation of a large number of institutes. It was funded by

The ECMWF analyses are distributed with special permission of D. Burridge. P. Bougeault, F. Lalaurette, J.F. Geleyn, V. Cassé, B. Lacroix, E. Legrand, J. Pailleux, B. Pouponneau and J.D. Gril, from Météo-France, contributed a lot to the achievement of the experiment, and to the formatting of the data. We also appreciate very much the help of A. Staniforth, J. Caveen, B. Bilodeau and C. Chouinard, from AES/RPN.

The PYREX experiment was made possible by the participation of a large number of institutes from France, Spain, and Germany. It was funded by Météo-France, the Instituto National de Meteorologia (Spain), the Institut National des Sciences de l'Univers (ARAT, PAMOS and PAMOY programs), the Centre National d'Etudes Spatiales, Electricité de France, Région Midi-Pyrénées, and the Deutsche Forschungsanstalt für Luft und Raumfahrt.

References

Bessemoulin, P., P., Bougeault, A. Genoves, A. Jansa Clar and D. Puech, 1993: Mountain pressure drag during PYREX. *Beitr. Phys. Atmosph.*, **66**, 305-325.

Bougeault, P., A. Jansa Clar, B. Benech, B. Carissimo, J. Pelon and E. Richard, 1997: PYREX:A summary of findings. *Bull. Amer. Meteor. Soc.*, **78**, 637-650.

Bougeault, P., A. Jansa, J.L. Attié, I. Beau, B. Benech, R. Benoit, P. Bessemoulin, J.L. Caccia, J. Campins, B. Carissimo, J.L. Champeaux, M. Crochet, A. Druilhet, P. Durand, A. Elkhalfi, P. Flamant, A. Genoves, M. Georgelin, K.P. Hoinka, V. Klaus, E. Koffi, V. Kotroni, C. Mazaudier, J. Pelon, M. Petitdidier, Y. Pointin, D. Puech, E. Richard, T. Satomura, J. Stein, and D. Tannhauser, 1993 : The atmospheric momentum budget over a major atmospheric mountain range: first results of the PYREX program. *Annales Geophysicae*, **11**, 395-418.

Bougeault, P., I. Beau and J. Stein, 1992: Validation of meteorological models and parameterization with observations of the PYREX field experiment. In *Validation of models over Europe, 7-11 September 1992, Reading* , pages 247-285. ECMWF.

Bougeault, P., A. Jansa Clar, B. Benech, B. Carissimo, J. Pelon and E. Richard, 1990: Momentum budget over the Pyrénées: The PYREX experiment. *Bull. Amer. Meteor. Soc.*, **71**, 806-818.

Campins, J.A., A. Jansà, B. Benech, E. Koffi, 1995 PYREX observation and diagnosis of the Tramontane wind. *Meteor. Atm. Phys.*, **56**, 209-228.

Clark, T.L. and M.J. Miller. Pressure drag and momentum fluxes due to the Alps Part II: Representation in large-scale atmospheric models. *Quart. J. Roy. Meteor. Soc.*, 117:527-552, 1991.

Durran D. R., 1990: Mountain wave and downslope winds. Atmospheric process over complex terrain, meteorological monographs. *Amer. Meteor. Soc.* **23**(45), 59-81.

Eliasen, A. and E. Palm, 1960: On the transfert of energy in stationary mountain waves. *Geophys. Norv.*, **22**, 1-23.

Georgelin, M., E. Richard, M. Petitdidier, and A. Druilhet, 1994: Impact of subgrid scale orography parameterization on the simulation of orographic flows. *Mon. Wea. Rev.*, **122**,

1509-1522.

Koffi, E., B. Benech, J. Stein and B. Terliuc, 1997: Characteristics of local flows around the Pyrenees in view of PYREX experiment data. Part II: Solution of an advanced linear theory model compared to field measurements. *J. Appl. Meteor.*, in press.

Lott, F., and M. J. Miller, 1997: A new sub-grid scale orographic drag parameterization: its formulation and testing. *Quart. J. Meteor. Soc.*, **123**, 101-127.

Masson, V., 1996: Numerical simulation of a low-level wind created by complex orography: A Cierzo case study. *Mon. Wea. Rev.*, **124**, 701-715.

Ölafsson, H. and P. Bougeault, 1996: Non linear flow past an elliptic mountain ridge. *J. Atmos. Sci.***53**(17), 2465-2489.

Mason, P.J., 1986: On the parameterization of the orographic drag. *E.C.M.W.F. workshop proc. on Fine scale modelling and the development of parameterization schemes, 275-288.*

Schär C. and D. R. Durran, 1997: Vortex formation and vortex shedding in continuously stratified flows past isolated topography. *J. Atmos. Sci.*, **54**, 534-554.

Smith, R.B., and V. Grubišić 1993: Aerial observation of Hawaii's wake. *J. Atmos. Sci.* , **50**, 3728-3750.

Smolarkiewicz, P.K., and R. Rotunno, 1990: Low Froude number flow past three-dimensional obstacles. Part I: Baroclinically generated lee vortices. *J. Atmos. Sci.*, **46**, 1154-1164.